# Determination of weak anisotropy parameters using traveltimes and polarisations.

*S. M. Soukina, D. Gajewski and B. M. Kashtan*

**email:** *soukina@dkrz.de*

**keywords:** *anisotropy, inversion, quasi-shear waves, traveltimes, polarisation*

## ABSTRACT

*Tomographic simultaneous inversion of quasi $P$- and $S$-waves in anisotropic media is a powerful tool to determine the elastic properties of the medium. Applying tomographic inversion in weakly anisotropic media for either $qP$- or $qS$-wave traveltimes alone allows to determine a limited number of elastic parameters. Only if $qP$- and $qS$-wave traveltimes are jointly inverted, the whole elastic tensor of the weakly anisotropic medium can be determined. The inversion of $qS$-wave traveltimes, however, leads to non-linear inversion relations. If also the observed $qS$-wave polarisation vectors are introduced into the inversion, the tomographic relations for $qS$-waves linearise and are formally identical to those for $qP$-waves. Numerical results for a homogeneous transversely isotropic (TI) model show that the full elastic tensor can be reconstructed and the elastic parameters of this tensor are in good accordance with the TI-medium under consideration. Inverting the full tensor of elastic parameters is useful if no a priori information on the symmetry and/or the orientation of the anisotropy system is available. If such information is available, a constrained inversion with a limited number of elastic parameters can be performed. An investigation of the sensitivity of the inversion with respect to errors in the orientation of the $qS$-wave polarisation vectors revealed that the inversion results are only slightly affected if errors of up to $25°$ are introduced.*

## INTRODUCTION

Anisotropic model building from surface seismic reflection data is a very challenging task since one has to deal with variations of the elastic parameters and the reflector depth simultaneously. If down-hole or cross-hole data are available, the inversion is less complicated since transmission data are considered. The basic relations for traveltime perturbations in weakly anisotropic media were established in 1982 (Červený, 1982; Hanyga, 1982). First applications of these formulae in an inversion scheme for $qP$-waves were published, e.g. by Červený and Jech (1982), who investigated transversely isotropic (TI) media with a non-vertical symmetry axis, or by Chapman and Pratt (1992) who considered arbitrary anisotropy, but restricted the inversion to 2-D wave propagation (i.e., rays remain in a plane containing the borehole). Most of the investigations published so far consider $qP$-waves. Jech and Pšenčík (1992) performed a joint inversion for $qP$- and $qS$-waves in TI media. For quasi-shear waves the relations for traveltime perturbations are intrinsically more complicated than for the quasi-compressional waves. In the homogeneous case the traveltime perturbations $\Delta\tau^{(M)}$ due to the perturbations of the elastic parameters $\Delta a_{iklm}$ read as follows (see e.g. Jech and Pšenčík, 1989; Červený, 2001):

$$\Delta\tau^{(M)} = -\frac{\tau_0}{2}\Delta a_{iklm}\, p_i^{(M)}\, p_m^{(M)}\, \mathrm{g}_k^{(M)}\, \mathrm{g}_l^{(M)}.$$

Here, $p_i^{(M)}$ and $\tau_0$ are components of the slowness vector and traveltime of the $S$-wave in the isotropic background medium. Indices $M = 1$ and 2 correspond to $qS1$- and $qS2$-waves. The traveltime perturbations $\Delta\tau^{(M)}$ depends on the polarisation vectors $\mathbf{g}^{(M)}$ in the background medium, which, in turn depend on the perturbations of the elastic parameters $\Delta a_{iklm}$. This leads to a non-linear behaviour of the $qS$-wave traveltime perturbations with respect to the perturbation of the elastic parameters. The polarisation of $P$-waves in the background medium corresponds to the phase normal which is known and, therefore, leads to linear perturbation relations.

Polarisation data provide additional information on the structure. The polarisation data can be used to invert for medium parameters as well as to improve the resolution of the tomographic image. Several papers using the polarisation tomography have been published. For instance, Le Bégat and Farra (1997) inverted $qP$-wave traveltimes and polarisations of synthetic examples simulating a VSP experiment. Horne and Leaney (2000) inverted $qP$- and $qSV$ polarisation and slowness component measurements obtained from a walk-away VSP experiment using a global optimisation method. Horne and MacBeth (1994) developed a genetic algorithm to invert shear-wave observations from VSP data. They used horizontal polarisations and time-delays to invert for hexagonal and orthorombic symmetry. The polarisation data were also used by Hu and Menke (1992), Farra and Le Bégat (1995), Holmes et al. (2000).

In this paper we will present a joint inversion of $qP$- and $qS$-waves in homogeneous weakly anisotropic media using a linear inversion formalism for both $qP$- and $qS$-waves. The observed $qS$-wave polarisation vectors are used to approximate vectors $\mathbf{g}^{(M)}$, $(M = 1, 2)$. With the known vectors $\mathbf{g}^{(M)}$ the relations between the traveltime perturbations and the perturbations of elastic parameters become linear and formally identical to the relations for $qP$-waves. This allows to use the same inversion scheme for $qP$- as for $qS$-waves. We assume that each of the two propagating $qS$-waves are recorded separately, i.e., no $qS$-wave coupling, and that the observations are not close to singular directions. The traveltimes and polarisations of $qS$-waves on three-component seismic records can usually be determined by Alford rotation (see e.g Alford, 1986; Li and Crampin, 1993; Dellinger et al., 1998).

After this introduction we briefly review the required basic perturbation formulae, followed by the inversion scheme used in this study. Special emphasis is given to the determination of the vectors $\mathbf{g}^{(M)}$ for the inversion using the polarisation vectors of $qS$-waves. Numerical inversion examples demonstrate the applicability of the scheme where also the sensitivity to errors in the polarisation vector is discussed.

## BASIC PERTURBATION FORMULAE

We consider homogeneous weakly anisotropic media and use the high-frequency approximation of the wave field. In the case of weak anisotropy the tensor of the elastic parameters is represented by a sum of the tensor of the density-normalised elastic parameters in an isotropic background medium, $a^{(iso)}_{iklm}$, and small perturbations $\Delta a_{iklm}$ describing the deviations from isotropy:

$$a_{iklm} = a^{(iso)}_{iklm} + \Delta a_{iklm}. \tag{1}$$

It is furthermore assumed that the perturbations $\Delta a_{iklm}$ are formally considered to be of the same order as $\omega^{-1}$, where $\omega$ is the circular frequency.

For media of weak anisotropy the zeroeth-order solution for the wave field of $qP$- and $qS$-waves is written in the following form (see Červený, 2001; Zillmer et al., 1998; Pšenčík, 1998):

$$\mathbf{u}^{qP} = \frac{e^{-i\omega\tau_p}}{\sqrt{\rho J_p(\tau,\gamma_1,\gamma_2)}} D(\gamma_1,\gamma_2)\, e^{i\omega\Delta\tau_{qP}}\, \mathbf{n}(\gamma_1,\gamma_2) \tag{2}$$

$$\mathbf{u}^{qS} = \frac{e^{-i\omega\tau_s}}{\sqrt{\rho J_s(\tau,\gamma_1,\gamma_2)}} \left[A(\gamma_1,\gamma_2)\, e^{i\omega\Delta\tau_{qS1}}\, \mathbf{g}^{(1)}(\gamma_1,\gamma_2) + C(\gamma_1,\gamma_2)\, e^{i\omega\Delta\tau_{qS2}}\, \mathbf{g}^{(2)}(\gamma_1,\gamma_2)\right].$$

Here, $\mathbf{u}^{qP}$ and $\mathbf{u}^{qS}$ are displacement vectors of $qP$- and $qS$-waves, and $\tau_p$ and $\tau_s$ are traveltimes of the $P$- and $S$-waves in the isotropic background medium, respectively (bold letters denote vectors); $J_p$ and $J_s$ are Jacobians of the transformation from ray coordinates $(\tau,\gamma_1,\gamma_2)$ to Cartesian coordinates. The scalar amplitudes $A$, $C$ and $D$ are defined by the initial conditions, e.g., by the type of the source (see e.g. Gajewski, 1993).

In equation (2), the traveltime perturbation $\Delta\tau_{qP}$ is:

$$\Delta\tau_{qP} = -\frac{\tau_p}{2}\Delta a_{iklm} p_i p_m n_k n_l, \tag{3}$$

where $\mathbf{p}$ is the slowness vector and $\mathbf{n} = v_p^2\,\mathbf{p}$ is the unit vector tangent to the reference ray of the $P$-wave in the isotropic background medium.

In equation (3), the traveltime perturbations $\Delta\tau_{qS1}$ and $\Delta\tau_{qS2}$ are obtained by the formulae

$$\Delta\tau_{qS1} = -\frac{\tau_s}{2}\,\lambda_1, \tag{4}$$

$$\Delta\tau_{qS2} = -\frac{\tau_s}{2}\,\lambda_2, \tag{5}$$

where $\lambda_1$ and $\lambda_2$ are eigenvalues of the weak-anisotropy matrix

$$B_{IM} = \Delta a_{iklm} p_k p_m e_i^{(I)} e_l^{(M)}, \qquad (I, M = 1, 2). \tag{6}$$

Also in equation (3,) the mutually orthogonal unit vectors $\mathbf{g}^{(1)}$ and $\mathbf{g}^{(2)}$ are linear combinations of the arbitrary mutually orthogonal unit vectors $\mathbf{e}^{(1)}$ and $\mathbf{e}^{(2)}$ situated in a plane perpendicular to the reference $S$-wave ray in the isotropic background medium, i.e.,

$$\mathrm{g}_i^{(1)} = e_i^{(1)}\cos\phi + e_i^{(2)}\sin\phi, \quad \mathrm{g}_i^{(2)} = -e_i^{(1)}\sin\phi + e_i^{(2)}\cos\phi. \tag{7}$$

The linear combinations (7) are constructed from the eigenvectors $(\cos\phi, -\sin\phi)^{\mathrm{T}}$ and $(\sin\phi, \cos\phi)^{\mathrm{T}}$ corresponding to the eigenvalues $\lambda_1$ and $\lambda_2$ of the weak-anisotropy matrix (6). For more details see Červený (2001), Jech and Pšenčík (1989), Zillmer et al. (1998), Pšenčík (1998). For the inversion we will use equations (4) and (5) for the traveltime perturbations in the form

$$\Delta\tau_{qS1} = -\frac{\tau_s}{2}\,\Delta a_{iklm}\,p_i\,p_m\,\mathrm{g}_k^{(1)}\,\mathrm{g}_l^{(1)}, \tag{8}$$

$$\Delta\tau_{qS2} = -\frac{\tau_s}{2}\,\Delta a_{iklm}\,p_i\,p_m\,\mathrm{g}_k^{(2)}\,\mathrm{g}_l^{(2)}. \tag{9}$$

## SYNTHETIC VSP EXPERIMENT

We computed three-component seismograms for the following observation scheme (see Figure 1). A borehole is situated at the point $X = 0.5$ km and $Y = 0$ km of a Cartesian coordinate system with horizontal $X-$ and $Y-$axes and a vertical $Z-$axis which is parallel to the borehole. 25 receivers are distributed along the borehole with a spacing of 30 m. Three types of waves propagating in a homogeneous transversely isotropic medium with a vertical axis of symmetry (VTI) are recorded at the receivers. The wave fields are generated at nine different source positions on the surface $Z = 0$, where tilted unit forces are used as sources. The tilted forces have a fixed orientation $\mathbf{F}$ for all source positions such that the orientation is given by

$$\mathbf{F} = (\sin\theta\cos\varphi, \sin\theta\sin\varphi, \cos\theta), \quad \text{where} \quad \theta = 45^\circ, \varphi = 45^\circ. \tag{10}$$

Synthetic seismograms at the receivers were computed using standard anisotropic ray tracing (see e.g. Gajewski and Pšenčík, 1988). We consider two homogeneous VTI models which differ only in the strength of anisotropy. The density-normalised elastic parameters are given in Table 1. The corresponding isotropic background models are obtained from an iteration procedure described below using the formulae for the best-fitting isotropic medium derived by Fedorov (1968). The orientation of the receivers in the borehole coincides with the general Cartesian coordinate system, i.e., the two horizontal components are aligned with the $X-$ and $Y-$axes and the vertical component points along the $Z-$axis. Examples of the three-component seismograms for the source positions 1, 3 and 6 (see Figure 1) are shown in Figure 2.

The traveltimes $\tau_{qP}$, $\tau_{qS1}$ and $\tau_{qS2}$ and the unit polarisation vectors $\mathbf{A}_{qP}$, $\mathbf{A}_{qS1}$ and $\mathbf{A}_{qS2}$ computed using standard anisotropic ray tracing for each receiver serve as observed data. Using these data we want to recover the perturbations of the elastic parameters $\Delta a_{iklm}$, where we assume that an initial isotropic background model, $a_{iklm}^{(iso)}$, is known.

## SCHEME OF INVERSION

For the inversion we use a system of equations formed by the equations (3), (8) and (9) corresponding to the different source–receiver combinations, where the traveltime perturbations, the slowness vectors and

Weak Anisotropy (WA), 5%

$$\begin{pmatrix} 13.59 & 6.79 & 6.12 & 0. & 0. & 0. \\ & 13.59 & 6.12 & 0. & 0. & 0. \\ & & 12.23 & 0. & 0. & 0. \\ & & & 3.06 & 0. & 0. \\ & & & & 3.06 & 0. \\ & & & & & 3.40 \end{pmatrix}$$

Weak Anisotropy (WA), 10%

$$\begin{pmatrix} 13.59 & 6.80 & 5.44 & 0. & 0. & 0. \\ & 13.59 & 5.44 & 0. & 0. & 0. \\ & & 10.87 & 0. & 0. & 0. \\ & & & 2.72 & 0. & 0. \\ & & & & 2.72 & 0. \\ & & & & & 3.40 \end{pmatrix}$$

Best-fitting isotropic media:

$v_p^{(iso)} = 3.59$ km/s  
$v_s^{(iso)} = 1.80$ km/s

$v_p^{(iso)} = 3.48$ km/s  
$v_s^{(iso)} = 1.75$ km/s

**Table 1:** Density-normalised elastic parameters of two homogeneous VTI models (in km$^2$/s$^2$). The models differ only in the strength of anisotropy. $v_p^{(iso)}$ and $v_s^{(iso)}$ are the velocities of the compressional and shear waves in the corresponding isotropic background media.

vectors $\mathbf{g}^{(M)}$, $(M = 1, 2)$ are determined from the observed data. Key issue is the determination of vectors $\mathbf{g}^{(M)}$ to obtain a linear perturbation formula.

For each source–receiver combination in the background isotropic medium traveltimes $\tau_p$ and $\tau_s$ and the slowness vectors of the compressional and shear waves are computed. The traveltime perturbations $\Delta\tau_{qP}$, $\Delta\tau_{qS1}$ and $\Delta\tau_{qS2}$ are the differences between the observed traveltimes $\tau_{qP}$, $\tau_{qS1}$, $\tau_{qS2}$ and the corresponding traveltimes $\tau_p$ and $\tau_s$ computed in the background medium. The vector $\mathbf{n}$ in equation (4) is the unit vector along the ray (slowness) in the isotropic background medium at the receiver. The polarisations $\mathbf{A}_{qS1}$ and $\mathbf{A}_{qS2}$ of the two quasi-shear waves are used to estimate the unknown vectors $\mathbf{g}^{(1)}$ and $\mathbf{g}^{(2)}$ needed in the perturbation formulae (8) and (9) by the following procedure. The observed polarisation vectors $\mathbf{A}_{qS1}$ and $\mathbf{A}_{qS2}$ are projected onto a plane orthogonal to the reference ray, i.e., orthogonal to $\mathbf{n}$. Although these projections $\tilde{\mathbf{A}}_{qS1}$ and $\tilde{\mathbf{A}}_{qS2}$ are usually not mutually orthogonal, we can use them to estimate the vectors $\mathbf{g}^{(1)}$ and $\mathbf{g}^{(2)}$. The unit vectors corresponding to $\tilde{\mathbf{A}}_{qS1}$ and $\tilde{\mathbf{A}}_{qS2}$ are denoted by $\tilde{\mathbf{g}}^{(1)}$ and $\tilde{\mathbf{g}}^{(2)}$. We now use these vectors $\tilde{\mathbf{g}}^{(1)}$ and $\tilde{\mathbf{g}}^{(2)}$ instead of the unknown vectors $\mathbf{g}^{(1)}$ and $\mathbf{g}^{(2)}$ to solve the

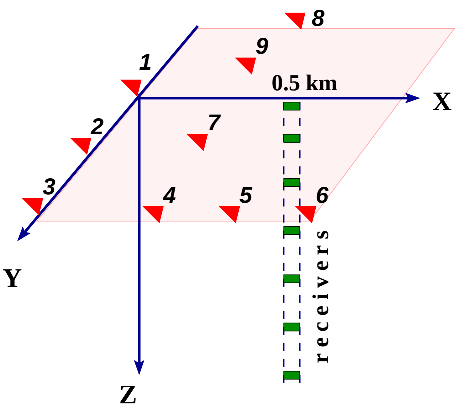


**Figure 1:** The observation scheme of the numerical experiment. A vertical borehole contains 25 aligned three-component receivers with 30 m spacing until a depth of 750 m. The source positions on the surface denoted by reference numbers are indicated by triangles. Sources represent a tilted unit force with fixed orientation for all shots (see eq. 10).

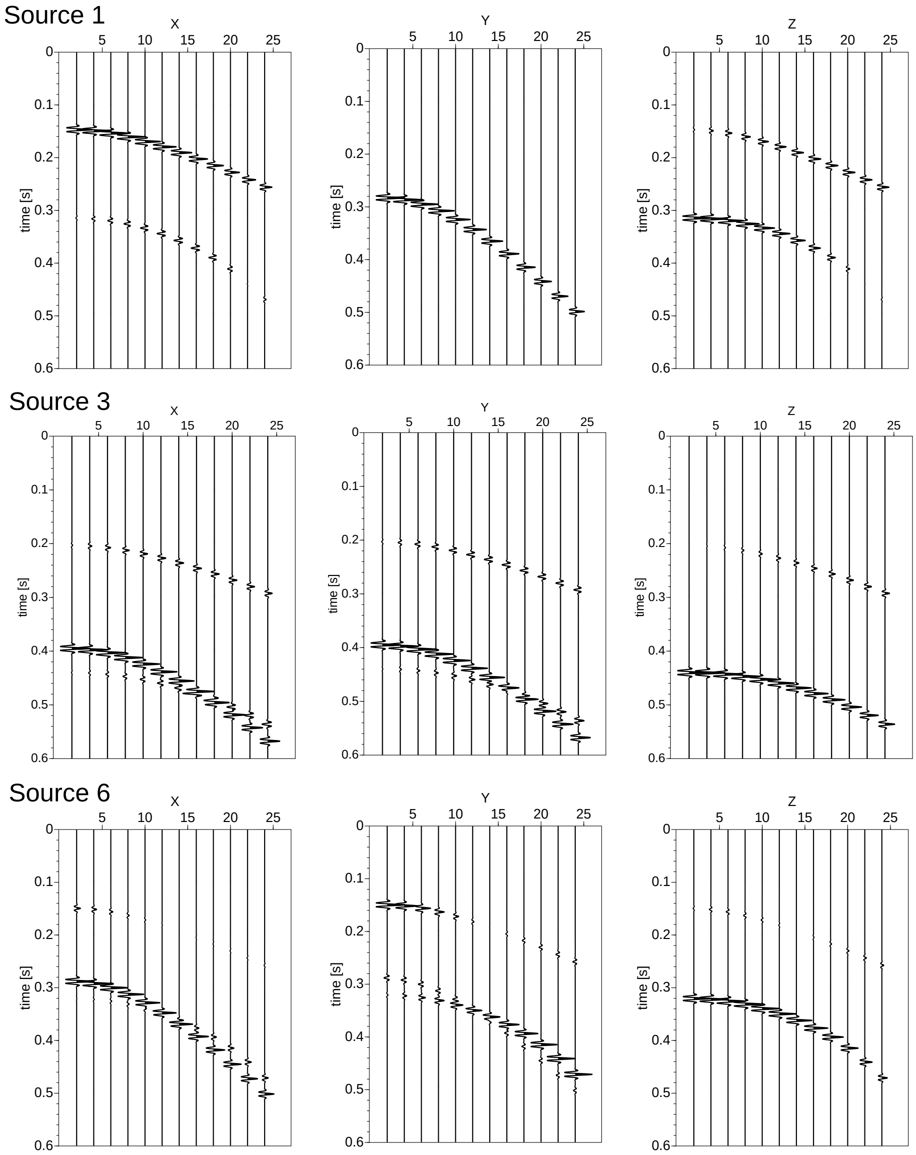


**Figure 2:** Synthetic three-component data for the source positions 1, 3 and 6 (see Fig. 1) for the model with 10% anisotropy. The vertical component is $Z$ (right), the horizontal components are $X$ and $Y$ (left and center). Orientations of $X$, $Y$ and $Z$ are along the axis of the general cartesian coordinate sytem. The traveltime is given on the vertical axis against the receiver number on the horizontal axis. Both split shear waves are visible for the sources at 3 and 6.

inverse problem, i.e, instead of (8) and (9) we use the relations:

$$\Delta\tau_{qS1} = -\frac{\tau_s}{2}\,\Delta a_{iklm}\, p_i\, p_m\, \tilde{g}_k^{(1)}\, \tilde{g}_l^{(1)}, \tag{11}$$

$$\Delta\tau_{qS2} = -\frac{\tau_s}{2}\,\Delta a_{iklm}\, p_i\, p_m\, \tilde{g}_k^{(2)}\, \tilde{g}_l^{(2)}. \tag{12}$$

The accuracy of this approximation is investigated below.

The tomographic system is constructed from the equations (3), (11) and (12) corresponding the different source-receiver combinations. The system can be written in a compact form:

$$\delta\mathbf{T} = \mathbf{F}\,\delta\mathbf{m}, \tag{13}$$

where the vector $\delta\mathbf{T}$ is formed by the traveltime perturbations $\Delta\tau_{qP}$, $\Delta\tau_{qS1}$ and $\Delta\tau_{qS2}$. The vector $\delta\mathbf{T}$ has a dimension $N$ of the total number of the $qP$- and $qS$-wave observations for all recevers from all sources. The vector $\delta\mathbf{m}$ of the perturbations of the elastic parameters $\Delta a_{iklm}$ has a dimension $L$. Here $L$ is equal to 21 if the full elastic tensor is inverted, and $L$ equal 5 if only five elastic parameters determinig the VTI medium are inverted (see Appendix). The $L \times N$ matrix $\mathbf{F}$ is constructed from the corresponding components of the slowness vectors, the vectors $\tilde{\mathbf{g}}^{(M)}$ or $\mathbf{n}$ and the traveltimes in the background medium (see eqs. 3, 11 and 12). The matrix $\mathbf{F}$ is a large, sparse matrix. Since number of the observations $N$ is greater then the number of seeked parameters $L$ the system (13) is overdetermined. To find the perturbations of the elastic parameters $\delta\mathbf{m}$ the singular value decomposition (SVD) technique is used. SVD produces a solution of system (13) that is the best approximation in the least-squares sence. SVD searches for $\delta\mathbf{m}$ that minimise $\chi^2$ such that:

$$\chi^2 = |\mathbf{F}\,\delta\mathbf{m} - \delta\mathbf{T}|^2.$$

## ACCURACY OF VECTORS $\tilde{\mathbf{g}}^{(M)}$

Under the assumption of weak anisotropy the orientations of all vectors $\mathbf{A}_{qSM}$, $\mathbf{g}^{(M)}$ and $\tilde{\mathbf{g}}^{(M)}$ $(M = 1, 2)$ are close to each other (see e.g. Jech and Pšenčík, 1989). The accuracy of this assumption is investigated in this section. To show how close these vectors are, the following test is carried out for the two models under consideration (see Table 1). For the construction of matrix $\mathbf{B}$ used in equation (6) we choose two arbitrary mutually orthogonal unit vectors $\mathbf{e}^{(1)}$ and $\mathbf{e}^{(2)}$ in the plane perpendicular to the reference ray in the following way:

$$\mathbf{e}^{(1)} = \frac{1}{\sqrt{n_3^2 + n_1^2}} \begin{pmatrix} n_3 \\ 0 \\ -n_1 \end{pmatrix}; \qquad \mathbf{e}^{(2)} = \mathbf{n} \times \mathbf{e}^{(1)}, \tag{14}$$

where $\times$ denotes the vectorial product and $\mathbf{n}$ is the unit vector tangent to the reference ray. These base vectors $\mathbf{n}$, $\mathbf{e}^{(1)}$ and $\mathbf{e}^{(2)}$ vary for each receiver position. For each receiver we compute the vectors $\mathbf{g}^{(M)}$, $(M = 1, 2)$ using the eigenvectors of matrix $\mathbf{B}$ (see eqs. 6 and 7) by solving the eigenvalue problem.

Here we will compare the components of the vectors $\mathbf{g}^{(M)}$ and the polarisation vectors $\mathbf{A}_{qSM}$ from the observed data with respect to the same coordinate system. This coordinate system is determined by the base vectors $\mathbf{n}$, $\mathbf{e}^{(1)}$ and $\mathbf{e}^{(2)}$. The components of $\mathbf{g}^{(M)}$ with respect to the base vectors $\mathbf{e}^{(1)}$ and $\mathbf{e}^{(2)}$ are known from equations (7). Since the vectors $\mathbf{g}^{(M)}$ are located in a plane perpendicular to the reference ray, they have no components along $\mathbf{n}$. Then, we compute the components of the polarisation vectors $\mathbf{A}_{qSM}$ with respect to the base vectors $\mathbf{n}$, $\mathbf{e}^{(1)}$ and $\mathbf{e}^{(2)}$. The components of $\mathbf{A}_{qSM}$ with respect to $\mathbf{e}^{(1)}$ and $\mathbf{e}^{(2)}$ are also the components of the projections $\tilde{\mathbf{A}}_{qSM}$ of $\mathbf{A}_{qSM}$ onto a plane orthogonal to the reference ray with respect to the same base vectors. The unit normalized projections $\tilde{\mathbf{A}}_{qSM}$ produce the vectors $\tilde{\mathbf{g}}^{(M)}$

Figure 3 shows the components of the vectors $\mathbf{g}^{(M)}$ (dotted lines) and the vectors $\mathbf{A}_{qSM}$ (solid lines) with respect to base vectors $\mathbf{n}$, $\mathbf{e}^{(1)}$ and $\mathbf{e}^{(2)}$. Those components are shown for all receivers in the model with 10% anisotropy for the sources 1, 3, and 6. Because the vectors $\mathbf{g}^{(M)}$ are perpendicular to $\mathbf{n}$, only the components of $\mathbf{g}^{(M)}$ with respect to base vectors $\mathbf{e}^{(1)}$ and $\mathbf{e}^{(2)}$ are displayed (i.e., two dotted lines in each plot). The three solid lines in each plot show the components of the vector $\mathbf{A}_{qSM}$ with respect to the base vectors. The solid lines without dots close to them are the components of the polarisation vectors $\mathbf{A}_{qSM}$ with respect to base vector $\mathbf{n}$. Due to the type of symmetry considered (i.e., VTI) one of the $qS$-waves has a pure $SH$ polarisation, therefore, its component in $\mathbf{n}$-direction vanishes (see plots on the left of Figure 3).

According to Figure 3 the components of $\mathbf{A}_{qSM}$ and the components of the vectors $\mathbf{g}^{(M)}$ with respect to base vectors $\mathbf{e}^{(1)}$ and $\mathbf{e}^{(2)}$ are very close to each other. It is means that the vectors $\tilde{\mathbf{g}}^{(M)}$ are close to the vectors $\mathbf{g}^{(M)}$. We conclude from this numerical test, that the normalised projections of the polarisation vectors $\mathbf{A}_{qSM}$ onto the plane perpendicular to the ray in the background medium provide good approximations for the vectors $\mathbf{g}^{(M)}$ $(M = 1, 2)$ needed in the perturbation formulae (8) and (9), i.e., the numerical test justifies the applicability of relations (11) and (12) instead of (8) and (9). Therefore, relations (11) and (12) will be used to invert the synthetic data.

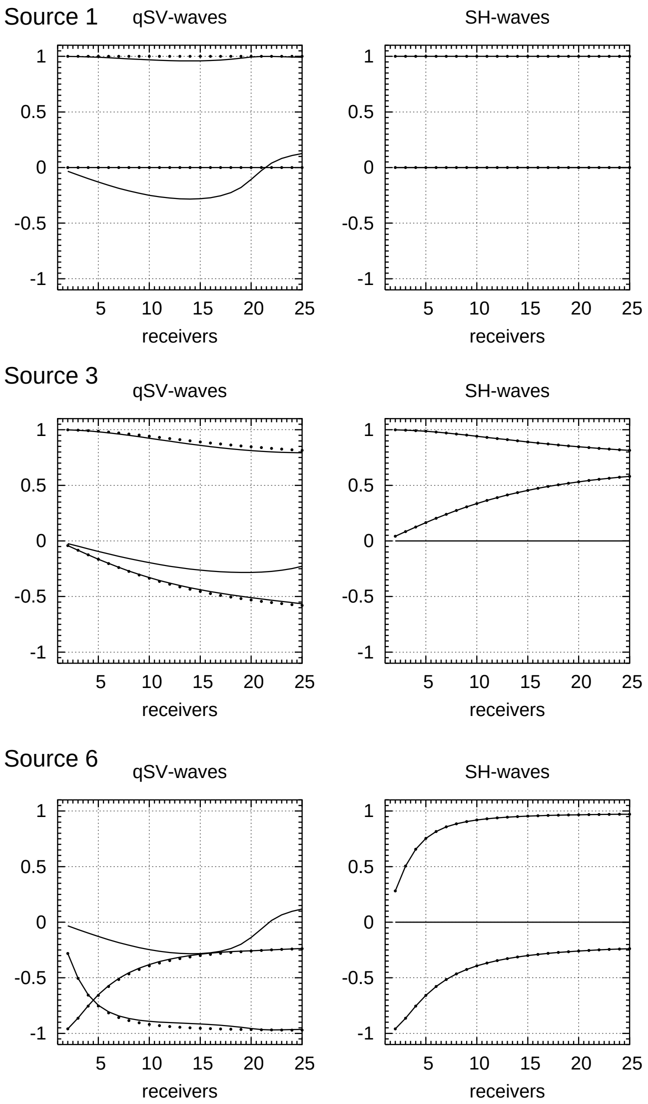


**Figure 3:** Components of the vectors $\mathbf{g}^{(M)}$ and the polarisation vectors $\mathbf{A}_{qSM}$ $(M = 1, 2)$ for the model with 10% anisotropy (see Tab. 1) estimated from the synthetic data with respect to the base vectors $\mathbf{n}$, $\mathbf{e}^{(1)}$ and $\mathbf{e}^{(2)}$. The vectors $\mathbf{g}^{(M)}$ and $\mathbf{A}_{qSM}$ are shown for all 25 receivers and sources 1, 3, and 6 (see Fig. 1). Solid lines represent components of $\mathbf{A}_{qSM}$. The components of $\mathbf{g}^{(M)}$ with respect to base vectors $\mathbf{e}^{(1)}$ and $\mathbf{e}^{(2)}$ are displayed by dots (for details, see the text).

## INVERSION OF SYNTHETIC VSP DATA

The inversion procedure is applied to two VTI models which differ in strength of the anisotropy (see Table 1). The isotropic reference models are constructed using the following iteration procedure. First, the velocities $v_p$ and $v_s$ estimated for several source-receiver pairs (i.e. as the distance divided by the corresponding traveltime) are used as parameters for the isotropic background medium. In the next step the elastic parameters determined by the inversion are used to construct an updated isotropic reference model using the formulae for the best-fitting isotropic medium derived by Fedorov (1968) (see also the Appendix). The inversion is repeated with the updated isotropic background model. The inversion and update of the isotropic background are repeated until the old velocities and the new velocities of the isotropic background differ only by a small value $\varepsilon$ (e.g., 0.01 km/s).

At the receivers the traveltimes of the three types of waves as well as the polarisation vectors $\mathbf{A}_{qS1}$, $\mathbf{A}_{qS2}$ are considered. First we assume that there are no errors in these data. To determine the elastic

Inversion for 21 elastic parameters:

$$\begin{pmatrix} 13.441 & 6.666 & 5.436 & 0.008 & 0.0111 & -0.004 \\ & 13.402 & 5.408 & -0.022 & -0.010 & -0.001 \\ & & 10.769 & 0.057 & -0.145 & 0. \\ & & & 2.625 & -0.022 & 0.016 \\ & & & & 2.664 & 0. \\ & & & & & 3.372 \end{pmatrix}$$

Inversion for 5 elastic parameters:

$$\begin{pmatrix} 13.432 & 6.653 & 5.372 & 0. & 0. & 0. \\ & 13.432 & 5.372 & 0. & 0. & 0. \\ & & 10.624 & 0. & 0. & 0. \\ & & & 2.627 & 0. & 0. \\ & & & & 2.627 & 0. \\ & & & & & 3.390 \end{pmatrix}$$

**Table 2:** Inversion results for the model with 10% anisotropy. The elastic parameters were determined using the inversion procedure for 21 parameters (left) and for 5 parameters (right). These parameters were used to compute the phase velocities shown in Figure 4 and 5.

Inversion for 21 elastic parameters:

$$\begin{pmatrix} 13.55 & 6.765 & 6.060 & 0.002 & 0.006 & -0.001 \\ & 13.544 & 6.054 & -0.006 & -0.004 & 0. \\ & & 12.220 & 0.015 & -0.042 & 0.001 \\ & & & 3.034 & -0.006 & 0.006 \\ & & & & 3.047 & 0. \\ & & & & & 3.393 \end{pmatrix}$$

Inversion for 5 elastic parameters:

$$\begin{pmatrix} 13.554 & 6.759 & 6.044 & 0. & 0. & 0. \\ & 13.554 & 6.044 & 0. & 0. & 0. \\ & & 12.179 & 0. & 0. & 0. \\ & & & 3.035 & 0. & 0. \\ & & & & 3.035 & 0. \\ & & & & & 3.397 \end{pmatrix}$$

**Table 3:** Inversion results for the model with 5% anisotropy. The elastic parameters were recovered using the inversion procedure for 21 parameters (left) and for 5 parameters (right). These parameters were used to compute the phase velocities shown in Figure 6 and 7.

parameters defining the weakly anisotropic medium we use $qP$-wave data as well as $qS$-wave data simultaneously. In weakly anisotropic media use of $qP$-wave data or $qS$-wave data alone allows to determine only 15 of the 21 elastic parameters (see, e.g., Pšenčík and Gajewski (1998) for $qP$-waves, and equations (16) and (17) of the Appendix for $qS$-waves). Only the joint inversion allows to determine the full elastic tensor of the medium.

For each source–receiver pair and each type of wave the traveltime differences $\Delta\tau_{qS1}$, $\Delta\tau_{qS2}$ and $\Delta\tau_{qP}$ between observed traveltimes and computed traveltimes in the isotropic background medium are considered. The vectors $\tilde{\mathbf{g}}^{(1)}$, $\tilde{\mathbf{g}}^{(2)}$ are obtained from the synthetic data as described above.

First, for both models the inversion for 21 parameters is performed, meaning that no a priori knowledge on the type and orientation of the anisotropy is assumed. The determined elastic parameters are shown in Tables 2 and 3 (left side). The parameters are close to the exact ones, but the type of symmetry is slightly different from VTI. However, the values of the "non-VTI" parameters, i.e., the off-diagonal elements except $A_{12}$, $A_{13}$ and $A_{23}$ are very small; $A_{11}$ is close to $A_{22}$ and $A_{44}$ is close to $A_{55}$ and $A_{13}$ is close to $A_{23}$, which indicates a medium of VTI symmetry. Figures 4 and 6 show the phase velocities computed from the inverted 21 elastic parameters and the exact model parameters.

Let us now assume that a priori information on the type and orientation of the anisotropy is available, i.e., we know that a VTI medium is under investigation. In this case we can restrict the inversion to five independent elastic parameters. The system of equations (3), (11) and (12) are specified under the assumptions of a VTI medium for the inversion. The results are presented in Tables 2 and 3 (right, see also Figure 5 and 7). The inversion results are close to the results of the inversion for 21 parameters. It is interesting to note that the phase velocities computed from the inverted 21 parameters for the $qP$- waves are even closer to the exact velocities than in the case of the inversion for 5 parameters. For the $qS$ wave phase velocities, the inversion of 5 parameters provides results which are slightly closer to the exact ones (Figure 8).

In the examples described above noise-free data were used. Because the exact vectors $\mathbf{g}^{(M)}$ and vectors $\tilde{\mathbf{g}}^{(M)}$ estimated from the synthetic polarisations almost coincide (see Figure 3), only negligable errors are introduced by this approximation in the examples shown. Since data from a VTI model are considered the illumination of the observation scheme used is sufficient to determine 21 parameters (where many of

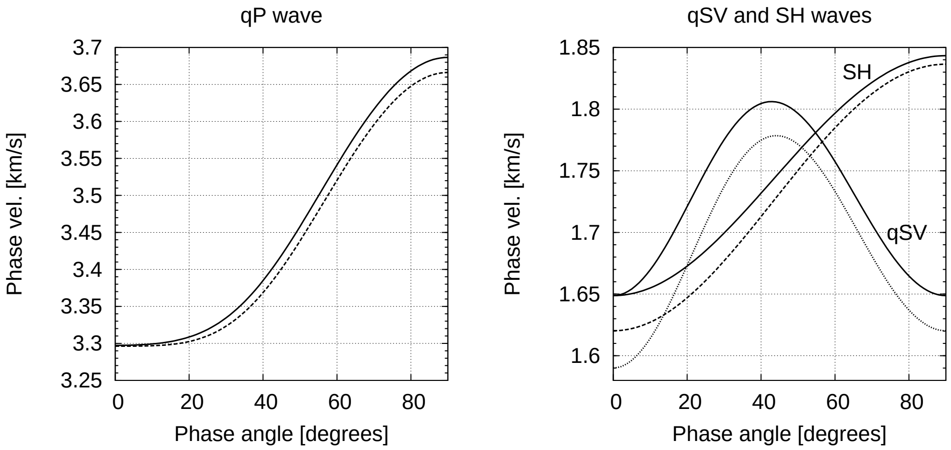


**Figure 4:** Exact and determined phase velocities following from the 21 inverted elastic parameters for the model with 10% anisotropy. Exact phase velocities are displayed by solid lines. Phase velocities computed from the determined parameters are shown by dashed lines for the $qP$-wave (left), and by dashed and dotted lines for $SH$- and $qSV$-waves, respectively (right).

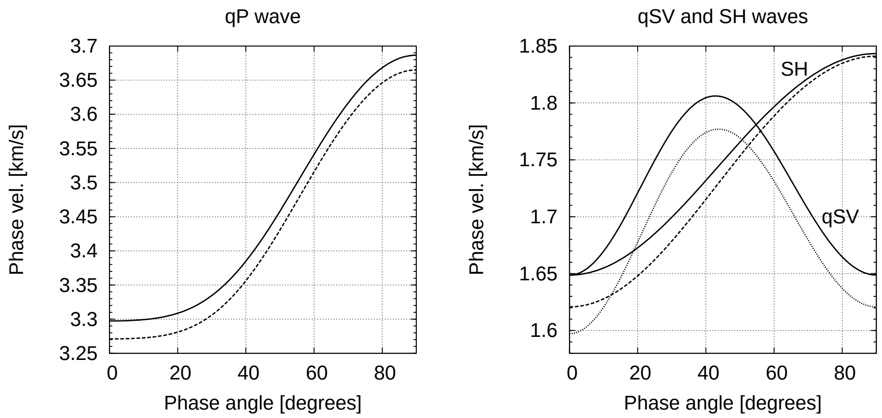


**Figure 5:** Exact and determined phase velocities following from 5 inverted elastic parameters for the model with 10% anisotropy. Exact phase velocities are displayed by solid lines. Phase velocities computed from the determined parameters are shown by dashed lines for the $qP$-wave (left), and by dashed and dotted lines for the $SH$- and $qSV$-waves, respectively (right).

them are almost zero). The quality of the inversion results thus mainly depends on the assumption of weak anisotropy. Therefore, the model with 5% anisotropy was recovered with higher accuracy than the model with 10% anisotropy (see Figure 8).

So far the data were considered to be free of errors. Now we examine the sensitivity of the inversion results to errors of the polarisation vectors. The unit polarisation vector **A** can be described by two angles: the inclination angle $\alpha$ and the azimuthal angle $\beta$:

$$\mathbf{A} = (\sin\alpha\,\cos\beta,\,\sin\alpha\,\sin\beta,\,\cos\alpha). \tag{15}$$

In the following examples we introduce errors into these two angles $\alpha$ and $\beta$ to perturb the orientation of the polarisation vector at each receiver position and for every shot. The errors are random with a normal (Gaussian) probability distribution and a mean value equal to zero and variance $\sigma$. To generate synthetic datas set with different noise levels the values of the variance $\sigma$ were altered from $10^\circ$ to $25^\circ$. Then, for each set of noisy polarisation data the inversion was performed. Figure 9 shows the results of inversions for all types of waves. According to these results the inversion procedure is not very sensitive with respect

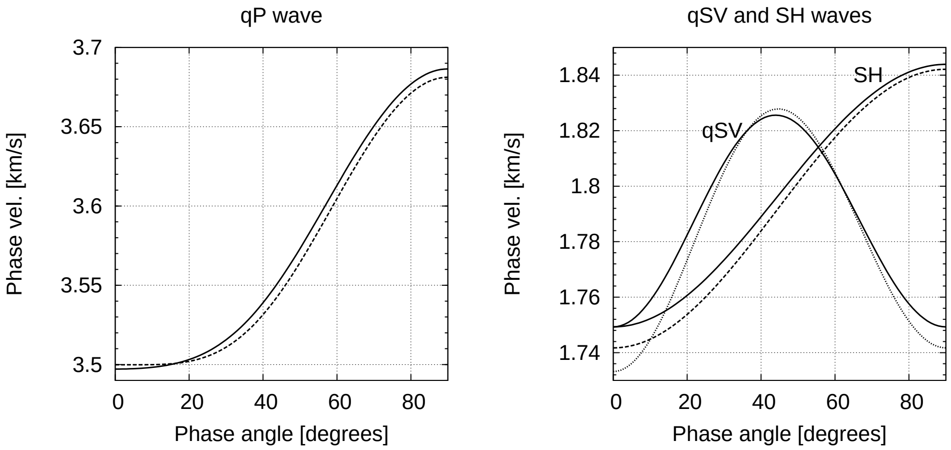


**Figure 6:** Exact and determined phase velocities following from 21 inverted elastic parameters for the model with 5% anisotropy. Exact phase velocities are displayed by solid lines. Phase velocities computed from the determined parameters are shown by dashed lines for the $qP$-wave (left), and by dashed and dotted lines for the $SH$- and $qSV$-waves, respectively (right).

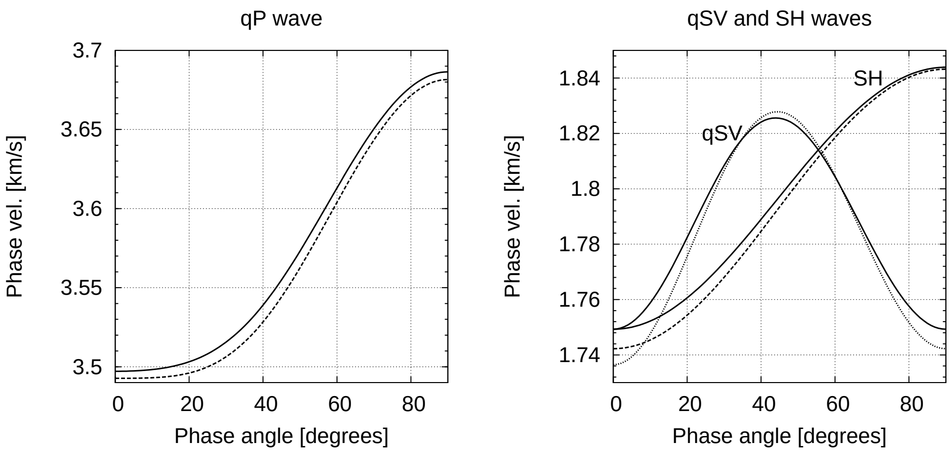


**Figure 7:** Exact and determined phase velocities following from 5 inverted elastic parameters for the model with 5% anisotropy. Exact phase velocities are displayed by solid lines. Phase velocities computed from the determined parameters are shown by dashed lines for the $qP$-wave (left), and by dashed and dotted lines for the $SH$- and $qSV$-waves, respectively (right).

to errors in the polarisation vectors of the order used in these examples. The results of the inversions of noisy polarisation data are close to the result of the inversion of noise-free data, even though the introduced errors are significant (a variance of $\sigma = 25°$).

## CONCLUSIONS

An inversion procedure for weakly anisotropic homogeneous elastic media using traveltimes of $qP$- and $qS$-waves as well as $qS$-wave polarisations was suggested. The presented inversion procedure allows to use the same linear inversion scheme for $qP$- as well as for $qS$-wave data. The joint inversion of $qP$- and $qS$-waves allows to determine the full elastic tensor if no a priory information on the type of symmetry and the orientation of the anisotropic medium is available.

The suggested procedure was tested on two homogeneous transversely isotropic models with a vertical axis of symmetry which differ in strength of the anisotropy (5% and 10%). Noisy and noise-free synthetic data were considered. For the considered models the full elastic tensor (21 elastic parameters) was deter-

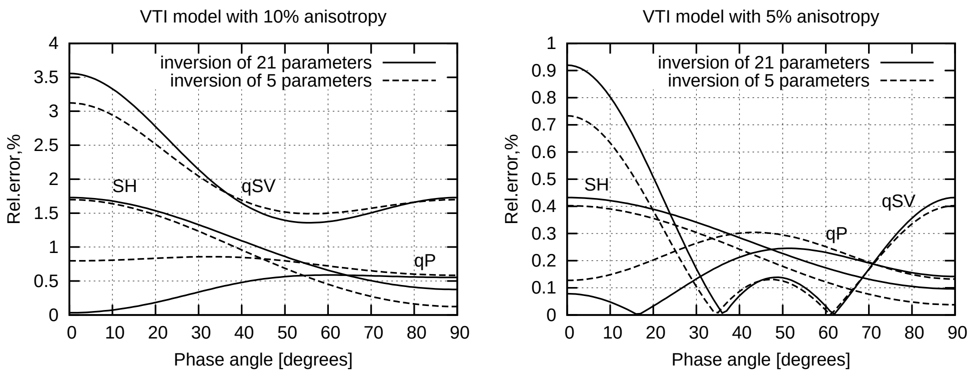


**Figure 8:** Relative errors of phase velocities for the three wave types $qP$, $SH$ and $qSV$ with respect to the exact velocities for the two VTI models: on the left side the model with 10% anisotropy, on the right side the one with 5% anisotropy (for the parameters see Tab. 1). Errors of the phase velocities $V$ obtained after inversion with respect to the exact phase velocities $V_{\text{exact}}$ are computed in percents (i.e., $100 * |V - V_{\text{exact}}|/V_{\text{exact}}$). Solid lines show the relative errors of the inversion for 21 elastic parameters; dashed lines show the relative errors after inversion for 5 elastic parameters.

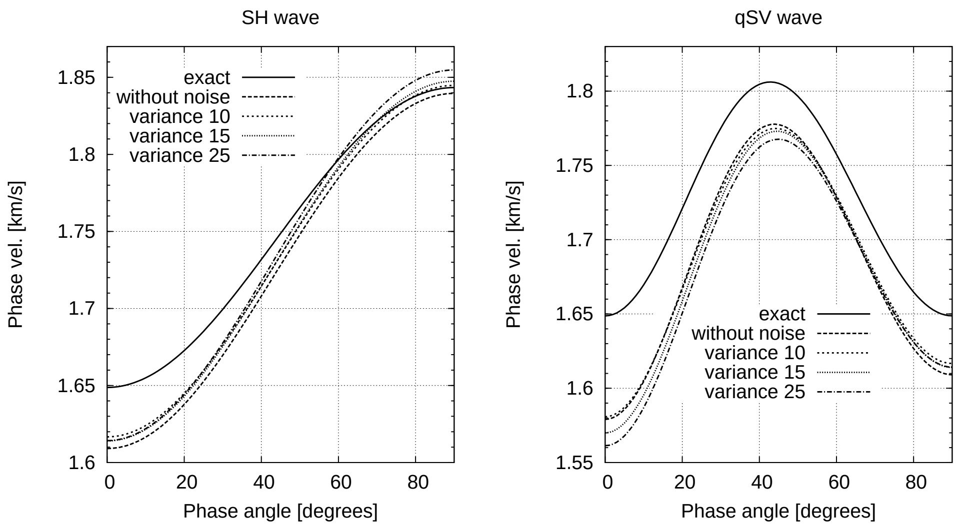


**Figure 9:** The results of the inversion for 5 parameters in the model with 10% anisotropy using noisy polarisation data. Noise was introduced into the polar angles defining the unit polarisation vectors (see text). Exact phase velocities are represented by solid lines. Long dashed lines display phase velocities after inversion of noise-free data, remaining lines represent phase velocities after inversions of noisy data with different variances of $\sigma = 10°$, $15°$ and $25°$.

mined with a sufficient accuracy. For the model with 5% of anisotropy the maximum deviations between the exact phase velosities and and phase velocites calculated from the inverted elastic parameters were below 1%. For the model with 10% of anisotropy the maximum relative errors of the phase velocites rise up to 3.5% for some directions. A constrained inversion (i.e., including a priori information) for 5 elastic parameters only slightly improved the results. For the numerical examples used in this investigation, the illumination of the observation scheme used was sufficient. In case of models with a lower symmetry (e.g., orthorhombic or triclinic) the issue of illumination is much more crucial and will require better walk away and azimuthal coverage and may even need crosshole observations to recover the full elastic tensor. This needs to be further studied. Tests of the sensitivity of the inversion results on errors in the polarisation vectors used in the inversion reveal an almost negligable influence. This results applies to the investigated models and error magnitudes of up to $25°$ in orientation.

The extension of the proposed method to heterogeneous media is not straight forward since the vectors $\mathbf{g}^{(M)}$ $(M = 1, 2)$ along the reference ray rotate because of two reasons: inhomogeneities of the isotropic background medium and changes of anisotropic parameters along the ray. The trade-off between anisotropy and inhomogeneities is a complicated problem. Therefore, the next step is the inversion of the elastic parameters of factorized anisotropic (FA) media (see Červený and Simões-Filho, 1991), where the rotations of the vectors $\mathbf{g}^{(M)}$ only depend on the inhomogeneities of the isotropic background medium. The rotation (or torsion) angle can be computed by established techniques (see, e.g., Červený, 2001). The described procedure would be applied for every segment of the ray starting at the receiver, and ending at the source where the rotation of the vectors $\mathbf{g}^{(M)}$ is taken into account by applying the proper rotation to the polarisation vector. Final results are then obtained by an integration along the ray. This will be the subject of future investigations.

## ACKNOWLEDGEMENTS

This research was partly supported by the German Research Foundation (DFG Ga 350/11-1), the sponsors of the Wave Inversion Technology (WIT) Consortium, the German Academic Exchange Service (DAAD) and the Russian Foundation of Fundamental Research (grant numbers 00-05-65083, 02-05-74022). We are grateful to the members of the Applied Geophysics Group for useful discussions and the improvement of the manuscript. The discussions on the content of this paper with I. Pšenčík are appreciated.

## REFERENCES

Alford, R. M. (1986). Shear data in the presence of azimuthal anisotropy. In *Expanded Abstracts*, page S9.6. Soc. Expl. Geophys.

Červený, V. (1982). Direct and inverse kinematic problems for inhomogeneous anisotropic media — a linearization approach. *Contr. Geophys. Inst. Sov. Acad. Sci.*, 13:127–133.

Červený, V. (2001). *Seismic ray theory*. Cambridge University Press.

Červený, V. and Jech, J. (1982). Linearized solutions of kinematic problems of seismic body waves in inhomogeneous slightly anisotropic media. *Geophys. J. Int*, 51:96–104.

Červený, V. and Simões-Filho, I. A. (1991). The traveltime perturbations for seismic body waves in factorized anisotropic inhomogeneous media. *Geophys. J. Int*, 107:219–229.

Chapman, C. H. and Pratt, R. G. (1992). Traveltime tomography in anisotropic media — I. Theory. *Geophys. J. Int*, 109:1–19.

Dellinger, J., Nolte, B., and Etgen, J. (1998). Symmetric Alford diagonalization. In *Expanded Abstracts*, pages 1673–1676. Soc. Expl. Geophys.

Farra, V. and Le Bégat, S. (1995). Sensitivity of $qP$-wave traveltimes and polarization vectors to heterogeneity, anisotropy and interfaces. *Geophys. J. Int.*, 121:371–384.

Fedorov, F. I. (1968). *Theory of elastic waves in crystals*. Plenum Press, New York.

Gajewski, D. (1993). Radiation from point sources in general anisotropic media. *Geophys. J. Int.*, 113:299–317.

Gajewski, D. and Pšenčík, I. (1988). Ray synthetic seismograms for a 3-D anisotropic lithospheric structure. *Phys. Earth Planet. Interiors*, 51:1–23.

Hanyga, A. (1982). The kinematic inverse problem for weakly laterally inhomogeneous anisotropic media. *Tectonophysics*, 90:253–262.

Holmes, G. M., Crampin, S., and Young, R. P. (2000). Seismic anisotropy in granite at the Underground Research Laboratory, Manitoba. *Geophysical Prospecting*, 48:415–435.

Horne, S. and Leaney, S. (2000). Short note: Polarization and slowness component inversion for TI anisotropy. *Geophysical Prospecting*, 48:779–788.

Horne, S. and MacBeth, C. (1994). Inversion for seismic anisotropy using genetic algorithms. *Geophysical Prospecting*, 42:953–974.

Hu, G. and Menke, W. (1992). Formal inversion of laterally heterogeneous velocity structures from P-wave polarization data. *Geophys. J. Int.*, 110:63–69.

Jech, J. and Pšenčík, I. (1989). First-order perturbation method for anisotropic media. *Geophys. J. Int*, 99:369–376.

Jech, J. and Pšenčík, I. (1992). Kinematic inversion for qP and qS waves in inhomogeneous hexagonally symmetric structures. *Geophys. J. Int*, 108:604–612.

Le Bégat, S. and Farra, V. (1997). $P$-wave traveltime and polarization tomography of VSP data. *Geophys. J. Int.*, 131:100–114.

Li, X. Y. and Crampin, S. (1993). Linear-transform techniques for processing shear-wave anisotropy in four-component seismic date. *Geophysics*, 58:240–256.

Pšenčík, I. (1998). Green's functions for inhomogeneous weakly anisotropic media. *Geophys. J. Int*, 135:279–288.

Pšenčík, I. and Gajewski, D. (1998). Polarization, phase velocity, and NMO velocity of $qP$-waves in arbitrary weakly anisotropic media. *Geophysics*, 63:1754–1766.

Zillmer, M., Kashtan, B. M., and Gajewski, D. (1998). Quasi-isotropic approximation of ray theory for anisotropic media. *Geophys. J. Int.*, 132:643–653.

## APPENDIX A

In this Appendix we give explicit expressions for the perturbation equations for $qP$- and $qS$-waves as well as Fedorov's 1968 results on the best fitting isotropic approximations to abitrary anisotropic media.

The weakly anisotropic medium is given here in the compressed Voigt-notation $A_{\alpha\beta}$ for the density normalised tensor $a_{iklm}$ with the usual correspondence: $11 \to 1$, $22 \to 2$, $33 \to 3$, $23 \to 4$, $13 \to 5$, $12 \to 6$:

$$A_{\alpha\beta} = A^{(iso)}_{\alpha\beta} + \Delta A_{\alpha\beta}, \quad \alpha, \beta = 1, \ldots, 6 \quad ,$$

where $A^{(iso)}_{\alpha\beta}$ are the elastic parameters of the isotropic reference medium, and $\Delta A_{\alpha\beta}$ characterise the small deviations from the isotropic background medium.

The perturbation formula for $qP$-waves contains only 15 independent elastic parameters (or combinations of them). Equation (16) is analogous to the result from Pšenčík and Gajewski (1998) (their equation 17a), however, for a better correspondence with the results in equation (17) of $qS$-waves below we rewrite it here in the following form:

$$\begin{aligned} \Delta\tau_{qP} = -\frac{\tau_p}{2v_p^2}\Big[ & n_1^4\Delta A_{11} + 2n_1^2n_2^2\epsilon_1 + 2n_1^2n_3^2\epsilon_2 + 4n_1^2n_2n_3\epsilon_3 + 4n_1^3n_3\Delta A_{15} \\ & +4n_1^3n_2\Delta A_{16} + n_2^4\Delta A_{22} + 2n_2^2n_3^2\epsilon_4 + 4n_2^3n_3\Delta A_{24} + 4n_1n_2^2n_3\epsilon_5 \\ & +4n_1n_2^3\Delta A_{26} + n_3^4\Delta A_{33} + 4n_2n_3^3\Delta A_{34} + 4n_1n_3^3\Delta A_{35} + 4n_1n_2n_3^2\epsilon_6\Big], \end{aligned} \tag{16}$$

where $v_p$ is the $P$-wave velocity, $\tau_p$ is the traveltime of the $P$-wave and $\mathbf{n}$ is the unit vector tangent to the reference ray in the isotropic background medium; $\Delta\tau(qP)$ is the traveltime perturbation with respect to the traveltime $\tau_p$ caused by the perturbations in the elastic parameters $\Delta A_{\alpha\beta}$. In equation (16) the following notations are used:

$$\epsilon_1 = \Delta A_{12} + 2\Delta A_{66}, \quad \epsilon_2 = \Delta A_{13} + 2\Delta A_{55}, \quad \epsilon_3 = \Delta A_{14} + 2\Delta A_{56},$$

$$\epsilon_4 = \Delta A_{23} + 2\Delta A_{44}, \quad \epsilon_5 = \Delta A_{25} + 2\Delta A_{46}, \quad \epsilon_6 = \Delta A_{36} + 2\Delta A_{45}.$$

Similarly, also the perturbation formula for $qS$-waves depends only on 15 elastic parameters (or combinations of them), we obtain from equations (8) and (9):

$$\begin{aligned}\tau_{qS_M} = -\frac{\tau_s}{2}\Big[& p_2^2 \mathrm{g}_2^2 \delta_1 + 2p_2\mathrm{g}_2 p_3\mathrm{g}_3\delta_2 + 2p_2\mathrm{g}_2(p_2\mathrm{g}_3 + p_3\mathrm{g}_2)\delta_3 + \\ &+2p_2\mathrm{g}_2(p_1\mathrm{g}_3 + p_3\mathrm{g}_1)\delta_4 + 2p_2\mathrm{g}_2(p_1\mathrm{g}_2 + p_2\mathrm{g}_1)\delta_5 + p_3^2\mathrm{g}_3^2\delta_6 + \\ &+2p_3\mathrm{g}_3(p_2\mathrm{g}_3 + p_3\mathrm{g}_2)\delta_7 + 2p_3\mathrm{g}_3(p_1\mathrm{g}_3 + p_3\mathrm{g}_1)\delta_8 + \\ &+2p_3\mathrm{g}_3(p_1\mathrm{g}_2 + p_2\mathrm{g}_1)\delta_9 + (p_2\mathrm{g}_3 + p_3\mathrm{g}_2)^2\Delta A_{44} + \\ &+2(p_2\mathrm{g}_3 + p_3\mathrm{g}_2)(p_1\mathrm{g}_3 + p_3\mathrm{g}_1)\Delta A_{45} + \\ &+2(p_2\mathrm{g}_3 + p_3\mathrm{g}_2)(p_1\mathrm{g}_2 + p_2\mathrm{g}_1)\Delta A_{46} + \\ &+2(p_1\mathrm{g}_3 + p_3\mathrm{g}_1)(p_1\mathrm{g}_2 + p_2\mathrm{g}_1)\Delta A_{56} + \\ &+(p_1\mathrm{g}_3 + p_3\mathrm{g}_1)^2\Delta A_{55} + (p_1\mathrm{g}_2 + p_2\mathrm{g}_1)^2\Delta A_{66}\Big], \quad M = 1,2.\end{aligned} \tag{17}$$

Here, $\tau_s$ is the traveltime of the $S$-wave in the isotropic background medium, $\Delta\tau(qS_M)$ is the traveltime perturbation with respect to the traveltime $\tau_s$ caused by the perturbations in the elastic parameters $\Delta A_{\alpha\beta}$, $\mathrm{g_i}$ is the $i$-component of the polarisation vector $\mathbf{g}^{(M)}$ of the $qS_M$ wave, see equation (7). For simplicity we omit the index $M$ in the following. In equation (17) the following notations are used:

$$\begin{aligned}&\delta_1 = \Delta A_{22} + \Delta A_{11} - 2\Delta A_{12}, \qquad \delta_2 = \Delta A_{23} + \Delta A_{11} - \Delta A_{12} - \Delta A_{13}, \\ &\delta_3 = \Delta A_{24} - \Delta A_{14}, \qquad \delta_4 = \Delta A_{25} - \Delta A_{15}, \qquad \delta_5 = \Delta A_{26} - \Delta A_{16}, \\ &\delta_6 = \Delta A_{33} + \Delta A_{11} - 2\Delta A_{13}, \qquad \delta_7 = \Delta A_{34} - \Delta A_{14}, \\ &\delta_8 = \Delta A_{35} - \Delta A_{15}, \qquad \delta_9 = \Delta A_{36} - \Delta A_{16}.\end{aligned}$$

In the case of a VTI medium formulae (16) and (17) take the following form:

$$\tau_{qP} = -\frac{\tau_p}{2v_p^2}\Big[(n_1^4 + n_2^4)\Delta A_{11} + n_3^4\Delta A_{33} + 2(n_2^2 n_3^2 + n_1^2 n_3^2)(\Delta A_{13} + 2\Delta A_{44})\Big]$$

$$\begin{aligned}\tau_{qS} = -\frac{\tau_s}{2}\Big\{ & \left[(p_2\mathrm{g}_3 + p_3\mathrm{g}_2)^2 + (p_1\mathrm{g}_3 + p_3\mathrm{g}_1)^2\right]\Delta A_{44} + \\ &+p_3^2\mathrm{g}_3^2(\Delta A_{11} + \Delta A_{33} - 2\Delta A_{13}) + +(p_1\mathrm{g}_2 + p_2\mathrm{g}_1)^2\Delta A_{66}\Big\}, \quad M = 1,2,\end{aligned}$$

where $\tau_p$ and $\tau_s$ are the traveltimes of the $P$- and $S$-waves in the isotropic background medium; $v_p$ is the $P$-wave velocity in the isotropic background; $\Delta\tau(qP)$ and $\Delta\tau(qS)$ are the traveltime perturbations with respect to the corresponding traveltime $\tau_p$ or $\tau_s$ caused by the perturbations in the VTI elastic parameters. These results show that for the VTI medium only three of the 5 independent parameters are present in the perturbation formula if either $qP$- or $qS$-waves are considered alone (i.e., in an inversion only 3 parameters can be recovered if only $qP$- or $qS$-waves are considered).

## APPENDIX B

For the construction of reference isotropic models the formulae for the best-fitting isotropic medium derived by Fedorov (1968) were used:

$$v_s^2 = \frac{1}{30}\Big(3a_{ikik} - a_{iikk}\Big), \qquad v_p^2 = \frac{1}{30}\Big(3a_{iikk} - a_{ikik}\Big) + v_s^2. \tag{18}$$

Here $v_p$ and $v_s$ are the velocities of the $P$- and $S$-waves in the isotropic medium, $a_{iklm}$ are the density normalized elastic parameters of the anisotropic medium under consideration.